The Deformation Mechanisms of Superplasticity

H. W. HAYDEN, S. FLOREEN, AND P. D. GOODELL

Under various conditions of stress and temperature various deformation mechanisms could be rate-controlling for superplastic deformation. In general at low stresses diffusion creep should be rate-controlling. At temperatures between approximately 40 and 65 pct of the absolute melting point grain boundary diffusion should be the dominant diffusion path while at higher temperatures volume diffusion should dominate. At intermediate stresses, grain boundary sliding should be the major deformation mode, but the sliding rate should be governed by the lesser rate of dislocation creep within the grains. At temperatures between 40 and 65 pct of the melting point, the rate of dislocation creep should be controlled by dislocation pipe diffusion, while at higher temperatures volume diffusion should be rate-controlling. At high stresses the superplastic effect of unusually large tensile extensibility should diminish due to the greater possibility of work-hardening processes such as dislocation cell, tangle, and pile-up formation.

THE phenomenon of superplasticity has been observed in a wide variety of alloy systems. These include certain alloys of Bi,[1] Pb,[2-5] Sn,[6] Al,[7-11] Mg,[12] Fe,[13,14] Ni,[15,16] Ti,[17] and Zr.[17] There is general agreement that the superplastic effect of unusual tensile extensibility can be expected when an alloy having an extremely fine grain size is tested at a temperature in excess of 40 pct of the absolute melting point, and at strain rates where the flow stress is highly strain-rate sensitive.

The mechanical behavior of a superplastic material can be described by an equation of the form:

$$\dot{\gamma} = K\sigma^{1/m} d^{-A} D \qquad [1]$$

where $\dot{\gamma}$ is the strain rate, K a constant, σ the applied stress, d the grain size, D a diffusivity, m the strain rate exponent, and A the grain size exponent.

At very high stresses the observed deformation behavior is similar to the normal creep behavior of coarse-grained material and superplasticity is not observed. Values of m are typically less than 0.3. At intermediate stresses where fine-grained materials become superplastic, values of m ranging from 0.3 to 1.0 have been observed. A value of $m \doteq 0.5$ is typical of many alloys in the superplastic range. Frequently, but not always, m decreases at low stress levels.

Within the superplastic range the grain size exponent is often 2 or 3. From experimentally determined activation energies, the diffusivity appears to correspond to volume diffusion in some cases and to grain boundary (or dislocation pipe) diffusion in others.

At the present time there is controversy as to the deformation mechanisms of superplasticity. To date, theories have been based on: diffusion creep,[2,8] grain boundary sliding,[1,3-6,10-12,17-21] and dislocation climb and glide.[15,16,21,22] Although there are many pieces of experimental evidence in partial confirmation of each of these mechanisms, there is no single theory which can account for the many differences seen in the various alloys which have been reported.

In this paper, each of the possible deformation modes will be analyzed. Particular emphasis will be placed on differentiating between dominant observable processes and rate determining processes. The bulk of the analysis will be related to materials having equiaxed structures. A brief section will deal with materials having fibrous structures. New experimental evidence will then be presented and related to several of these analytical predictions.

H. W. HAYDEN, S. FLOREEN, and P. D. GOODELL are Research Associates and Metallurgist, respectively, The International Nickel Co., Paul D. Merica Research Laboratory, Sterling Forest, Suffern, N. Y.

Manuscript submitted September 9, 1971.

ANALYSIS

A) Vacancy Creep

Two theories of vacancy creep have been advanced. The first, involving volume diffusion, was originally proposed by Nabarro[23] and Herring.[24] The second, involving grain boundary diffusion, was proposed by Coble.[25] The creep rates predicted by these mechanisms are:

$$\dot{\gamma}_D = \frac{\alpha D_v \mathbf{b}^3 \sigma}{d^2 kT} \qquad [2]$$

$$\dot{\gamma}_D = \frac{\beta D_B \mathbf{b}^4 \sigma}{d^3 k T} \qquad [3]$$

where α and β are constant, D_v the volume diffusivity, D_B the grain boundary diffusivity, b the Burgers vector, d the grain size, k Boltzmann's constant, and T the absolute temperature. At high temperatures, a faster creep rate is predicted by the volume diffusion mechanism. At lower temperatures (T < 65 pct T_M), a faster creep rate is predicted by the grain boundary diffusion mechanism. For any condition, the process leading to the fastest creep rate will be effectively rate controlling.

Vacancy creep mechanisms have several inadequacies as sufficient explanations for superplasticity:

1) They predict a linear relation between stress and strain rate which is rarely observed.

2) The predicted strain rates are generally much lower than those observed experimentally.

3) Both mechanisms predict grain elongation which is rarely observed after extensive superplastic deformation.

It should be noted, however, that vacancy creep processes arise from a vacancy concentration gradient resulting from an applied stress. So long as there is no impediment to grain boundary displacements,[26] it is unlikely that there should be a limiting stress where they should cease operating. Thus in the limit where

the applied stress approaches zero, vacancy creep should become rate-controlling and the strain rate exponent should approach unity. Observations on several superplastic alloys show a trend toward decreased rather than increased strain rate exponents at low stresses. In the subsequent analysis and discussion, a reasonable basis for rationalizing the apparent contradiction between the above prediction and observations will be described. Studies on the deformation of coarse-grained copper and gold have shown a definite trend towards vacancy creep mechanisms at low stress levels.[27]

B) Grain Boundary Sliding

In coarse-grained polycrystalline materials, there is abundant evidence that the rate of grain boundary sliding is controlled by the rate of accommodating intragranular deformation processes. A recent analysis by Raj and Ashby[28] has shown that when the accommodation process is vacancy creep, the rate of grain boundary sliding and the rate of vacancy creep are identical. Similarly, when the accommodation process is dislocation creep, there are many indications that the rate of grain boundary sliding is controlled by the rate of intragranular creep. These have been summarized by Stevens:[29]

1) The rate of grain boundary sliding is usually proportional to the overall creep rate.

2) The activation energies for creep and sliding are the same and usually equivalent to the activation energies for volume diffusion.

3) Factors such as age hardening or phase transformations which have predictable effects on intragranular creep rates have comparable effects on grain boundary sliding.

The data of McLean and Gifkins[30] show that at high temperatures the percentage of strain from grain boundary sliding is independent of test temperature.

In the superplastic deformation of ultrafine-grained materials there is no reason to believe that the sliding rate is not controlled by the rate of intragranular deformation. In these materials a greater proportion of the total strain could arise from sliding, and the fine grain sizes might alter the mechanisms of grain deformation. We would suggest that rates of grain boundary sliding and dislocation creep are coupled, obeying a relationship of the form:

$$\dot{\gamma}_{GB} = \frac{K_1}{d}\dot{\gamma}_G \qquad [4]$$

where K_1 is an empirical constant. To the extent that the above suggestion is related to geometrical constraints, the value of K_1 should not change for various superplastic materials.

The above assumption should be applicable so long as the predicted sliding rates are less than the maximum possible sliding rates $(\dot{\gamma}_{GB})_{Max}$ based on grain boundary viscosity predicted by the Kê model[31,32]

$$(\dot{\gamma}_{GB})_{Max} = \frac{D_B \sigma \mathbf{b}^2}{dkT} \qquad [5]$$

where D_B is the grain boundary diffusivity, **b** the Burgers vector, and k Boltzmann's constant. Making appropriate substitutions in Eq. [5], the predicted strain rates are generally several orders of magnitude greater than those observed in superplastic deformation. Hence it is likely that the rate of grain boundary sliding is controlled by the rate of accommodation, Eq. [4], rather than by grain boundary viscosity, Eq. [5]. Similarly, it is unlikely that a tendency towards a maximum strain rate exponent at intermediate stresses could be explained by grain boundary viscosity limitations as has been suggested by Hart.[18]

C) Dislocation Creep

In general, superplasticity has been observed in materials having grain sizes less than 10 μ tested at temperatures greater than about 40 pct of the absolute melting point. The phenomenon occurs at low enough stress levels so that the expected dislocation cell size would be equal to or greater than the grain size (or a significant fraction thereof). Thus there is no cell formation.[5,15,16,21] At higher stresses where a cell structure would be expected and is produced,[15] there is a decrease in the sensitivity of flow stress to strain rate, indications of work-hardening[5,15] and a decrease in tensile elongation. At these higher stresses, the deformation behavior is similar to that of coarse-grained polycrystalline material.

On the basis of these observations, certain preconditions for any dislocation creep mechanism of superplasticity would seem reasonable:

1) Creep would occur without the formation of a dislocation cell structure. This would require that at any single time there be no more than three operative dislocation sources in any grain.[33]

2) Because of the very low stresses at which superplasticity can be observed, it is improbable that dislocation segments 10 μ or less in length would be sufficiently bowed out to act as Frank-Read sources. Consequently, dislocations are probably nucleated at grain corners or grain boundary ledges. Once nucleated they probably travel as reasonably straight segments by glide and climb. After traversing the grain, they are probably annihilated at suitable grain boundary locations.

3) Because of the low stresses, the absence of Frank-Read sources, and the great mobility of the grain boundaries for sliding[3-6,10-12,17,18] and migration,[34] it is improbable that dislocation pile-ups would be formed.

A dislocation creep mechanism for superplasticity involving the climb-controlled motion of edge dislocations has been proposed by Hayden and Brophy.[16] The analysis followed Weertman's[35] suggestion that the creep rate is the product

$$\dot{\gamma}_G = MA\mathbf{b}\,\frac{V}{H} \qquad [6]$$

where M is the number of active dislocation sources per unit volume, which would be on the order of one to three per grain, A is the average cross sectional area of a grain, V is the velocity of climb, and H is the distance a dislocation must climb above the plane of a potential dislocation source before the back stress from the dislocation is diminished to the point that a new dislocation may be nucleated.

The product of the first three terms of Eq. [6] is[16]

$$MA\mathbf{b} \approx \frac{\mathbf{b}}{d} \qquad [7]$$

Following Weertman's analysis, in absence of pile-up formation the height of climb should be

$$H = \frac{\mu \mathbf{b}}{6\pi(1-\nu)\sigma_e} \quad [8]$$

where μ is the shear modulus, ν is Poisson's ratio, and σ_e is the effective stress on a dislocation. In the earlier paper,[16] it was assumed that σ_e was identical to the applied stress. However, it is more likely that, at least in some cases, the effective stress on a dislocation should be

$$\sigma_e = \sigma - \sigma_0 \quad [9]$$

where σ_0 is either the stress necessary to nucleate a dislocation from a grain boundary source or the lattice friction stress.

In the earlier paper a parallel diffusion model for climb was assumed. It was further assumed that the average diffusion distance between dislocations and grain boundaries was $d/4$. However, it is more likely that there is little resistance to glide motion until the dislocations are quite close to the grain boundaries. Thus the average diffusion distance is probably not related to the grain size, but is instead in the order of about 10b. Furthermore it is unlikely that the back-stress affecting glide will have a similar effect on climb. The predicted climb velocity is then

$$V = \frac{D_v \mathbf{b}^2 \sigma}{10kT} \quad [10]$$

At intermediate temperatures there might be a greater flux of vacancies to dislocations via pipe diffusion than via volume diffusion. If so, then the diffusion path is the dislocation itself and the average diffusion distance should be approximately one-fourth the average dislocation length. This leads to a predicted climb velocity of[32]

$$V = \frac{4D_P \mathbf{b}^3 \sigma}{dkT} \quad [11]$$

where D_P is the pipe diffusivity. The temperature T_c at which the rate-controlling process would change from pipe to volume diffusion is that at which the two climb velocities are equal, or

$$T_c = \frac{Q_V - Q_P}{k \ln\left(\frac{D_{OV} d}{40 D_{OP} \mathbf{b}}\right)} \quad [12]$$

where D_{OV} and D_{OP} are the preexponential diffusion terms, and Q_V and Q_P are the activation energies for volume and pipe diffusion. At temperatures above T_c, the dislocation creep rate would be

$$\dot{\gamma}_G = \frac{6\pi(1-\nu)D_V \mathbf{b}^2 \sigma(\sigma - \sigma_0)}{10 d \mu kT} \quad [13]$$

Below T_c the dislocation creep rate would be

$$\dot{\gamma}_G = \frac{24\pi(1-\nu)D_P \mathbf{b}^3 \sigma(\sigma - \sigma_0)}{d^2 \mu kT} \quad [14]$$

These equations would apply for stresses at which the dislocation cell sizes would be greater than a significant fraction of the grain size.

At higher stresses above the upper limit, a dislocation cell structure should be formed and strain rate should vary with the fourth to seventh power of stress.[35]

D) A Combined Relationship

On the basis of the foregoing analysis, the observed strain rate during superplastic deformation should be the sum of the separate strain rates of vacancy creep, grain boundary sliding, and dislocation creep. At temperatures below T_c, Eq. [12], grain boundary diffusion should be rate-controlling for vacancy creep and pipe diffusion for dislocation creep. At temperatures above T_c volume diffusion should be rate-controlling for both vacancy and dislocation creep. The following creep relationships would be predicted:

$T < T_c$

$$\dot{\gamma}_{GB} = \frac{K_1}{d}\dot{\gamma}_G < (\dot{\gamma}_{GB})_M$$

$$\dot{\gamma}_T = \beta \frac{D_B \mathbf{b}^4 \sigma}{d^3 kT} + \left(\frac{K_1}{d} + 1\right) \frac{24\pi(1-\nu)D_P \mathbf{b}^3 \sigma(\sigma - \sigma_0)}{d^2 \mu kT} \quad [15]$$

$T < T_c$

$$\dot{\gamma}_{GB} = (\dot{\gamma}_{GB})_M$$

$$\dot{\gamma}_T = \beta \frac{D_B \mathbf{b}^4 \sigma}{d^3 kT} + \frac{D_B \sigma \mathbf{b}^2}{dkT} + \frac{24\pi(1-\nu)D_P \mathbf{b}^3 \sigma(\sigma - \sigma_0)}{d^2 \mu kT} \quad [16]$$

$T > T_c$

$$\dot{\gamma}_{GB} = \frac{K_1}{d}\dot{\gamma}_G < (\dot{\gamma}_{GB})_M$$

$$\dot{\gamma}_T = \alpha \frac{D_V \mathbf{b}^3 \sigma}{d^2 kT} + \left(\frac{K_1}{d} + 1\right) \frac{24\pi(1-\nu)D_V \mathbf{b}^2 \sigma(\sigma - \sigma_0)}{10 d \mu kT} \quad [17]$$

$T > T_c$

$$\dot{\gamma}_{GB} = (\dot{\gamma}_{GB})_M$$

$$\dot{\gamma}_T = \alpha \frac{D_V \mathbf{b}^3 \sigma}{d^2 kT} + \frac{D_B \sigma \mathbf{b}^2}{dkT} + \frac{6\pi(1-\nu)D_V \mathbf{b}^2 \sigma(\sigma - \sigma_0)}{10 d \mu kT} \quad [18]$$

At low stress levels at any temperature, vacancy creep would be the predominant and rate-controlling mechanism. At higher stress, in fine-grained materials, grain boundary sliding would be the predominant mechanism while dislocation creep would be rate-controlling. At still higher stresses, if the grain boundaries are not sufficiently viscous to allow sliding to keep up with grain strain, dislocation creep could become the predominant and rate-controlling mechanism. As discussed earlier, it is highly unlikely that this latter possibility would be observed. Table I shows the effective dependence of strain rate on stress, grain size, and activation energy where $\sigma \gg \sigma_0$ and $K_1/d \gg 1$.

E) Fibrous Grain Structures

In cases of materials where one grain dimension, L, is much greater than the other two, d, different super-

Table I. Effective Stress, Grain Size and Diffusion Dependencies for Superplastic Flow of Equiaxed Materials for Various Stress, Grain Boundary, and Temperature Conditions

$\dot{\gamma}_T \sim \sigma^A d^{-B} e^{-Q/RT}$

Temperature	Stress	Grain Boundary	A	B	Q*
$<T_c$	Low	Fully Viscous	1	3	Q_{GB}
$>T_c$	Low	Fully Viscous	1	2	Q_V
$<T_c$	Intermediate	Fully Viscous	2	3	Q_P
$>T_c$	Intermediate	Fully Viscous	2	~2	Q_V
$<T_c$	Intermediate	Limited Viscosity	2	2	Q_P
$>T_c$	Intermediate	Limited Viscosity	2	~1	Q_V
$<T_c$	High	–	4 to 7	–	Q_P
$>T_c$	High	–	4 to 7	–	Q_V

*Subscripts V = Volume Diffusion, GB = Grain Boundary, P = Pipe Diffusion.

plastic behavior might be expected than that for equiaxed structures. Since boundaries at about 45 deg to the maximum stress axis slide most freely, the ratio of sliding rate to grain strain rate should be sensitive to sample orientation. If the stress axis is parallel or normal to the fiber axis, the ratio should be proportional to the reciprocal of grain length, L. If the stress axis is at 45 deg to the fiber axis the ratio should be proportional to the reciprocal of the grain thickness, d.

When the grain length greatly exceeds the thickness, the expected dislocation cell size may be greater than the thickness but less than the length. Since cell size usually varies with the reciprocal of the applied stress,[36] it would be expected that a dislocation cell structure would form so as to divide the long axis of the grain. After formation of the cell structure the individual subgrains would be free to rotate with respect to each other. With continued straining, as the angle of misorientation between subgrains increases, the subboundaries should gradually approach the characteristics of high-angle grain boundaries. Inasmuch as such a process requires an increase in grain boundary area it should occur only as a means towards lowering the strain energy of the system. To the extent that the development of a finer grain size would permit greater ease for grain boundary sliding, this process would lead to a lowering of strain energy.

In predicting the creep rate for fibrous structures, the assumption for dislocation source density should be modified over that for equiaxed structures. In the latter case it was assumed that there should be one to three sources per grain. In the case of fibrous structures there should be about three sources per subgrain, or

$$M = \frac{12}{\pi d^2 d_c} = \frac{12\sigma}{\pi K_3 d^2} \qquad [19]$$

where K_3 is a constant relating the cell size, d_c, and the applied stress. The area swept out by a dislocation would be $\pi d^2/4$. The relationships for the height and velocity of climb should be the same as Eqs. [8], [10], and [11]. Combining these relationships, the dislocation creep rates should be

$$\text{at } T > T_c \qquad \dot{\gamma}_G = \frac{18\pi(1-\nu)D_V \mathbf{b}^2\sigma^2(\sigma-\sigma_0)}{10K_3\mu kT} \qquad [20]$$

$$\text{at } T < T_c \qquad \dot{\gamma}_G = \frac{72\pi(1-\nu)D_p \mathbf{b}^3\sigma^2(\sigma-\sigma_0)}{K_3 d\mu kT} \qquad [21]$$

Neglecting a small vacancy creep contribution, for sample oriented either parallel or normal to the fiber axis the observed creep rate should be

$$\dot{\gamma}_T = \left(\frac{K_1}{L} + 1\right)\dot{\gamma}_G \qquad [22]$$

For samples oriented 45 deg to the fiber axis the creep rate should be

$$\dot{\gamma}_T = \left(\frac{K_1}{d} + 1\right)\dot{\gamma}_G \qquad [23]$$

EXPERIMENTAL

A) Material Preparation

The three alloys whose compositions are shown in Table II were studied. All were vacuum melted and cast as 30 lb. 4 in. by 4 in. ingots.

Table II. Compositions of Materials Investigated

Alloy	Fe	Ni	Cr	Cu	Al	Ti
Ni-Base	26.2	Bal	34.9	–	–	0.58
IN-744	Bal	6 5	26	–	0.05	0.2
Fe-Cu	Bal	–	–	50	–	–

The nickel-base alloy was hot-rolled from 2300°F to $\frac{5}{8}$ in. bar stock. Samples of the bar stock were annealed 2 hr at 1800°F; 48 hr at 1800°F; or 100 hr at 1850°F plus 100 hr at 1800°F to produce the microstructures shown in Fig. 1.

Samples of IN-744 were prepared in two ways. Material having a reasonably equiaxed grain structure was taken from plate material which had been rolled from a 4 by 4 in. ingot to 2 in. thickness from 2300°F, reheated to 1700°F and rolled to $\frac{5}{8}$ in. thickness. Samples were tested in either the as-hot worked condition or after 1 hr anneals at either 1700°, 1800°, 1900°, or 2000°F. These latter annealing treatments were used to produce coarser grain sizes than those obtained in the as-worked stock. Material having an elongated grain structure was taken from bar stock rolled to 2 by 2 in. from 2300°F, reheated to 1700°F and rolled to $\frac{5}{8}$ in. sq. This material was tested in the as-hot worked condition.

Samples of 50-50 Fe-Cu were taken from $\frac{5}{8}$ in. sq bar stock which had been hot-rolled from 1700°F. These samples were tested in the as-hot worked condition.

B) Experimental Results

1) NICKEL-BASE ALLOY

The superplastic behavior of two-phase nickel-base alloys has been described earlier.[15,16] At temperatures between 1400° and 1800°F, the strain rate was proportional to the second power of stress divided by the second power of grain size over a wide range of stress. The activation energy of 60 kcal/mole was comparable to that expected for volume diffusion in nickel-base alloys.[38] These findings agree with the predictions for the model involving a dislocation climb process controlled by volume diffusion. In the present investigation testing was extended to lower temperatures to see if an activation energy comparable to that of pipe diffusion and the grain size sensitivity predicted by the pipe diffusion process would, in fact, be observed.

Fig. 2 presents the results of tensile tests between 1400° and 1800°F and creep tests between 1200° and 1400°F for samples of the nickel-base alloy having a grain size of 4.8 μ. There was a broad range of conditions where stress was proportional to the square root of strain rate, similar to earlier findings.[15,16] An Arrhenius plot based on this data is shown in Fig. 3. Between 1800° and ~1400°F the apparent activation energy is 61,000 cal per mole which is in excellent agreement with the value of 60,000 cal per mole reported in Ref. 15. Between ~1400° and 1200°F the activation energy was 36,000 cal per mole. This latter value is in reasonable agreement with published values for both grain boundary diffusion in nickel[38] and dislocation pipe diffusion in nickel.[39,40]

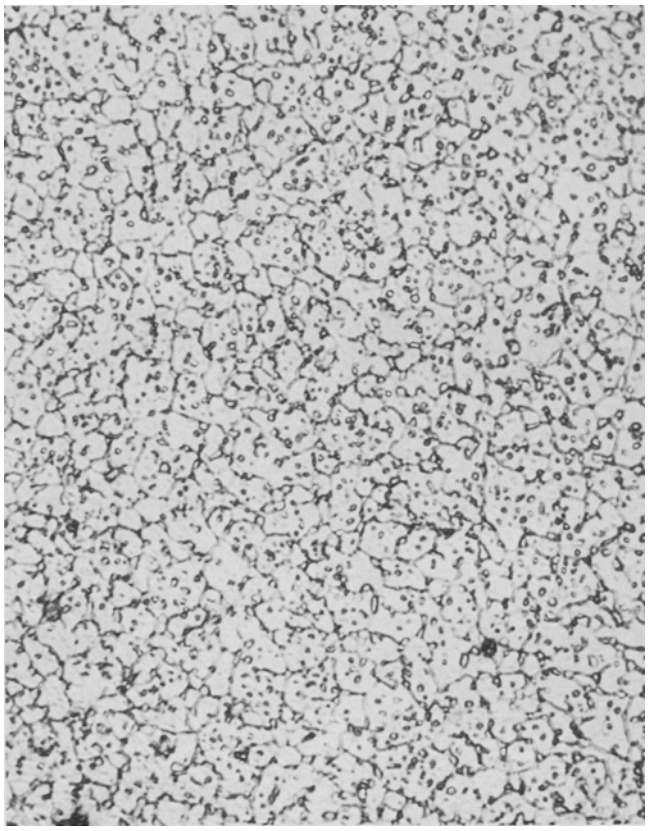

(a)

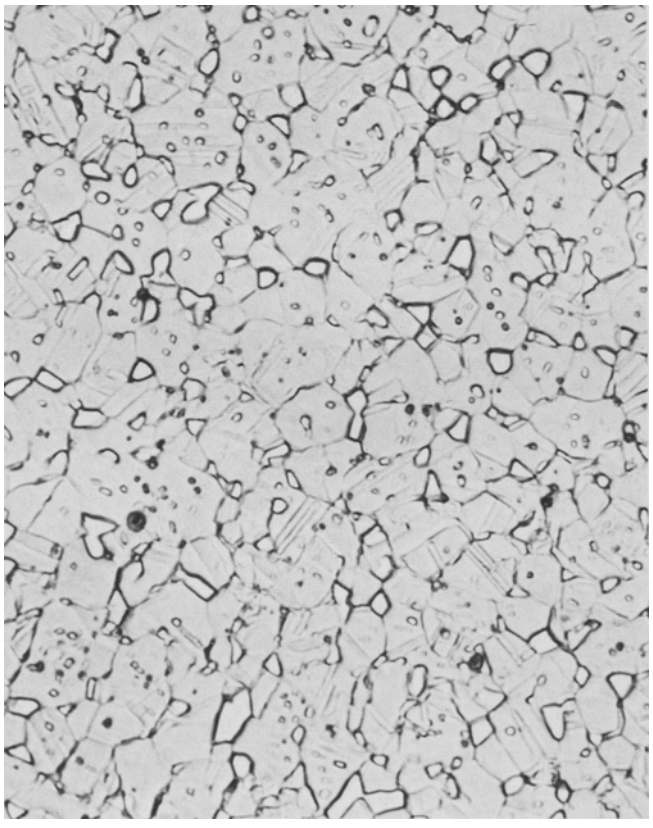

(b)

Fig. 1—Microstructures of nickel-base alloy samples. (*a*) Annealed 2 hr at 1800°F, magnification 1125 times; (*b*) annealed 48 hr at 1800°F, magnification 1125 times; (*c*) annealed 100 hr at 1850°F + 100 hr, 1800°F, magnification 845 times. All samples electrolytically etched in 50 pct H_3PO_4.

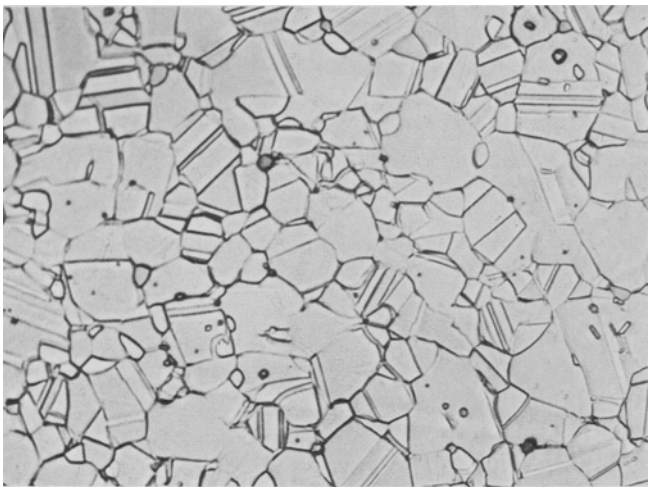

(c)

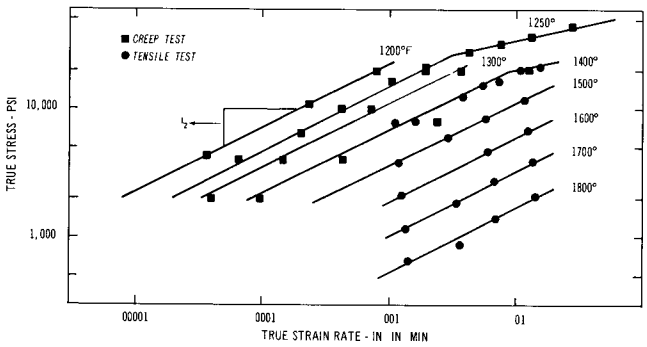

Fig. 2—Stress-strain rate data for a two-phase nickel-base alloy at various temperatures (°F).

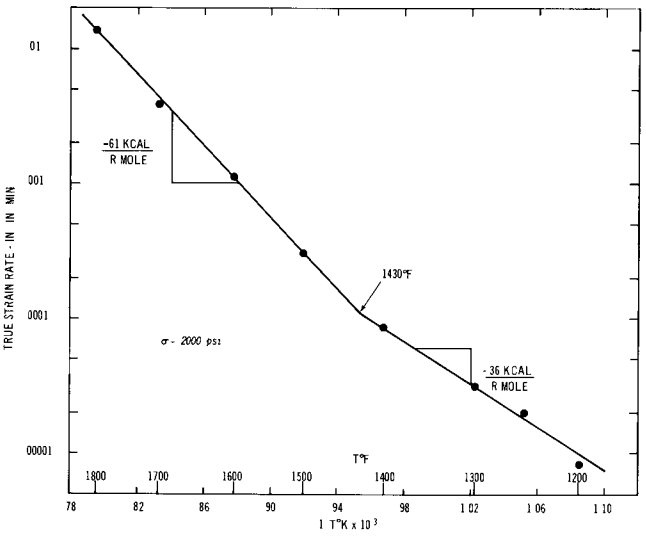

Fig. 3—Arrhenius plot based on the data of Fig. 2.

Fig. 4 shows the strain rates measured at several applied stresses in creep tests at 1400°, 1300°, and 1250°F for samples having grain sizes of 4.8, 8.3, and 13.5 μ. Over this temperature range strain rate was proportional to the reciprocal of the third power of grain size rather than the second power grain size as was previously observed in tests at 1800°F.[16]

In the temperature range 1200° to 1400°F, the deformation behavior may be represented by the equation

$$\dot{\epsilon} \sim \frac{\sigma^2}{d^3} \exp\left(\frac{-Q_p}{kT}\right) \qquad [24]$$

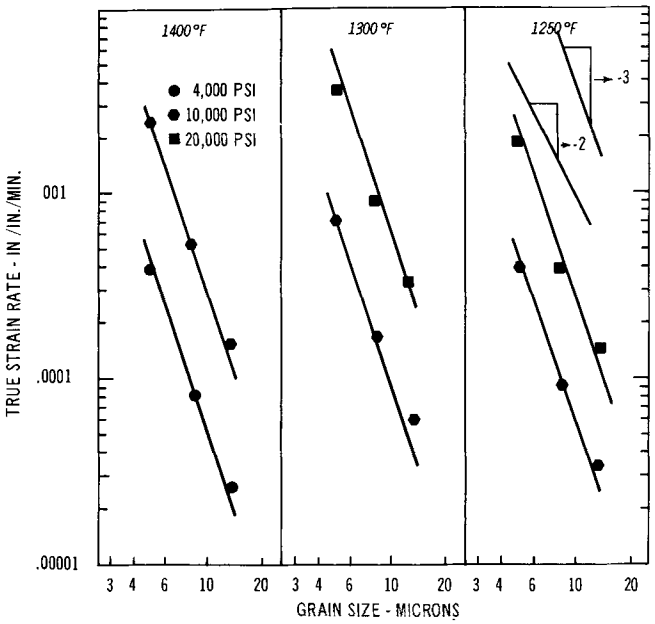

Fig. 4—The effect of grain size on strain rate at various stresses and temperatures.

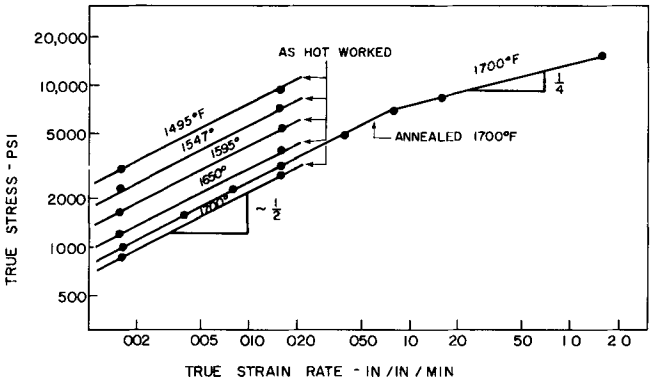

Fig. 5—Stress-strain rate data for samples of IN-744 having equiaxed grain structures.

The dependencies of strain rate on stress and grain size and the activation energy are all in agreement with the model based on dislocation pipe diffusion as the rate-controlling mechanism. Combining the present results of this investigation with those of previous studies of the superplastic behavior of two-phase nickel-base alloys leads to the following conclusions:

1) The rate of the predominant grain boundary sliding process is controlled by the rate of the lesser, though necessary, intragranular dislocation creep mechanism.

2) At temperatures above about 1400°F, volume diffusion is the rate-controlling process for dislocation creep, and hence for the overall deformation.

3) At temperatures below ~1400°F, dislocation pipe diffusion is the rate-controlling process for dislocation creep and hence for the overall deformation.

2) IN-744

Stress vs strain rate data at several temperatures for samples of IN-744 having equiaxed grain structures are shown in Fig. 5. Over a wide range of conditions stress was proportional to the square root of strain

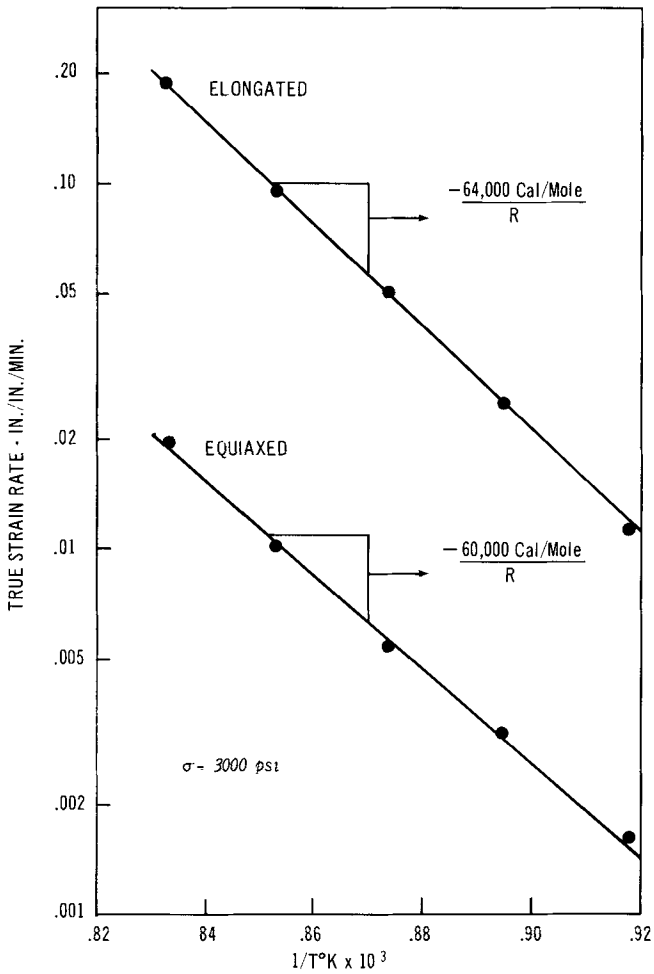

Fig. 6—Arrhenius plot based on stress-strain rate data for IN-744.

rate. An Arrhenius plot based on this data is shown in Fig. 6. The apparent activation energy of 60,000 cal/mole is in reasonable agreement with published values for volume diffusion in iron.[38] Fig. 7 shows that at 1700°F stress was linearly dependent on grain size at two different strain rates. Combining the results, the deformation behavior may be represented by the equation

$$\dot{\epsilon} \sim \left(\frac{\sigma}{d}\right)^2 \exp\left(-Q_d/kT\right) \qquad [25]$$

This functional relationship is the same as that for superplastic two-phase nickel-base alloys at temperatures above 1400°F. It is in agreement with the predictions of the model based on volume diffusion being the rate-controlling process.

Stress vs strain rate data for samples of IN-744 having fibrous grain structures are shown in Fig. 8. All of these data were obtained from a single sample using strain rate and temperature cycling procedures similar to those described in Ref. 15. The total plastic strain was less than 10 pct. In this material stress varied with the cube root rather than the square root of strain rate. The Arrhenius plot of these data, Fig. 6, gives an apparent activation energy of 64,000 cal/mole, in reasonable agreement with the 60,000 cal/mole value obtained for equiaxed material and also with published values for volume diffusion of iron.[38]

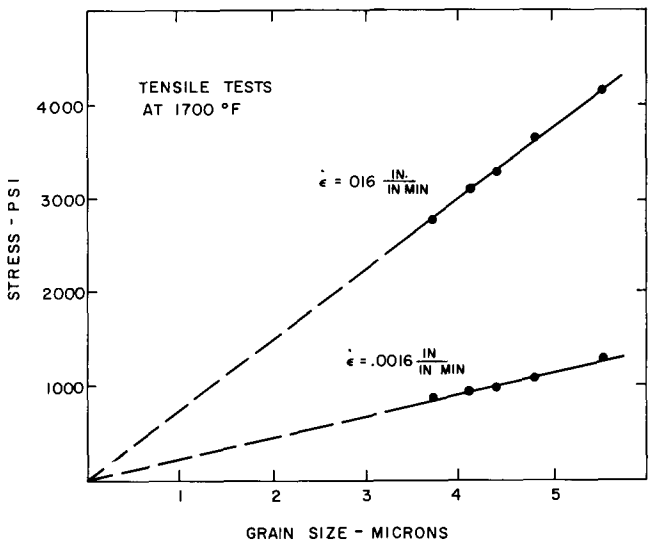

Fig. 7—The effect of grain size on the flow stress for IN-744 at two strain rates.

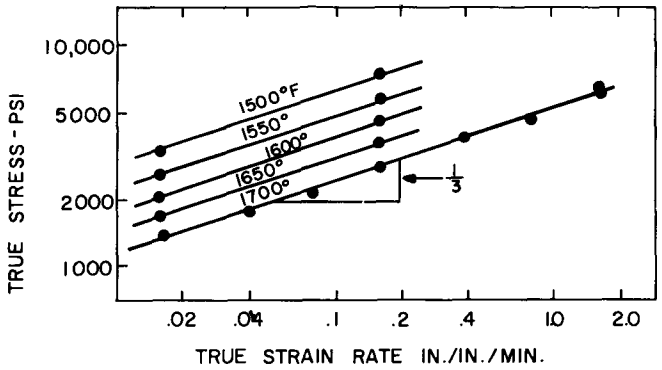

Fig. 8—Stress-strain rate data for IN-744 having an elongated grain structure.

The observed stress-strain rate relation and activation energy follow the model for longitudinal cell structure development through volume diffusion controlled dislocation climb.

Fig. 9 shows stress vs strain rate data for a single sample which was successively cycled between high and low crosshead speeds at 1700°F. It is evident that as the testing progressed the strain rate exponent gradually increased from $\frac{1}{3}$ to $\frac{1}{2}$. The exponent of $\frac{1}{2}$ was established after about 80 pct total plastic strain. Continued cycling at larger plastic strains caused no further change in the strain rate exponent. It is also apparent from Fig. 9 that deformation led to strain softening, particularly at the lower strain rates. Examination of deformed tensile samples revealed that this process was accompanied by a significant change in microstructure. The micrographs in Fig. 10 are from the grip, flange, and gage sections of a tensile bar which had been deformed in the manner described above. The grip section of the tensile bar had a decidedly fibrous microstructure, while the flange and gage sections show a definite trend towards the development of an equiaxed structure. Similar changes in microstructure also were observed in tensile samples which were deformed at fixed crosshead speeds rather than at varying speeds.

Although the initial deformation behavior of samples

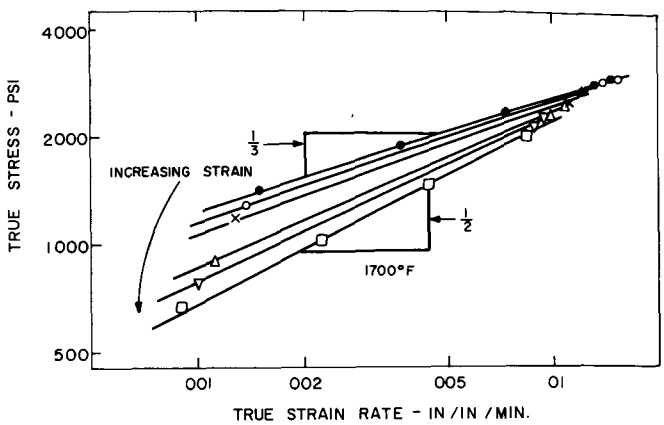

Fig. 9—The change in deformation behavior with increasing strain of a sample of IN-744 having an originally elongated grain structure.

having equiaxed and fibrous microstructures are different, the agreement of the activation energies suggests that the rate-controlling processes in both cases are the same, namely volume diffusion. The behavior of samples having originally fibrous structures suggests a continuous trend from the cell structure model to that appropriate to equiaxed structures. It seems highly unlikely that these observations could be rationalized by any mechanism not involving the formation of dislocation cells and subboundaries.

3) Fe-Cu

Stress vs strain-rate data for this alloy which had a fibrous grain structure are shown in Fig. 11. It can be seen that stress varies with strain rate to the 0.39 power. This exponent is somewhat in excess of the exponent of $\frac{1}{3}$ proposed in the model for fibrous structures. An apparent activation energy of 54,000 cal/mole has been calculated from these data, which is within the range of published values for the activation energies for volume diffusion in iron and copper.[38] Fig. 12 shows data for a single sample deformed at 1500°F where the crosshead speed was successively cycled between high and low rates. As in the case of fibrous IN-744 there was a trend towards increasing strain rate exponent with continued deformation. As before, once an exponent of 0.5 became established there was no further change with subsequent deformation. The grip, flange, and gage section microstructures shown in Fig. 13 are similar in their trend towards spheroidization to those of IN-744 shown in Fig. 10.

SUMMARY

The present results suggest that although grain boundary sliding may be a predominant deformation process in superplasticity its rate, and hence the overall deformation rate, is governed by intragranular dislocation climb.

The present results are functionally in agreement with the analytical models presented in this paper. The crucial test of the validity of these models is whether they will lead to quantitative predictions of the behavior of various superplastic alloys. As a means to this end the proportionality factor, K_1, between grain

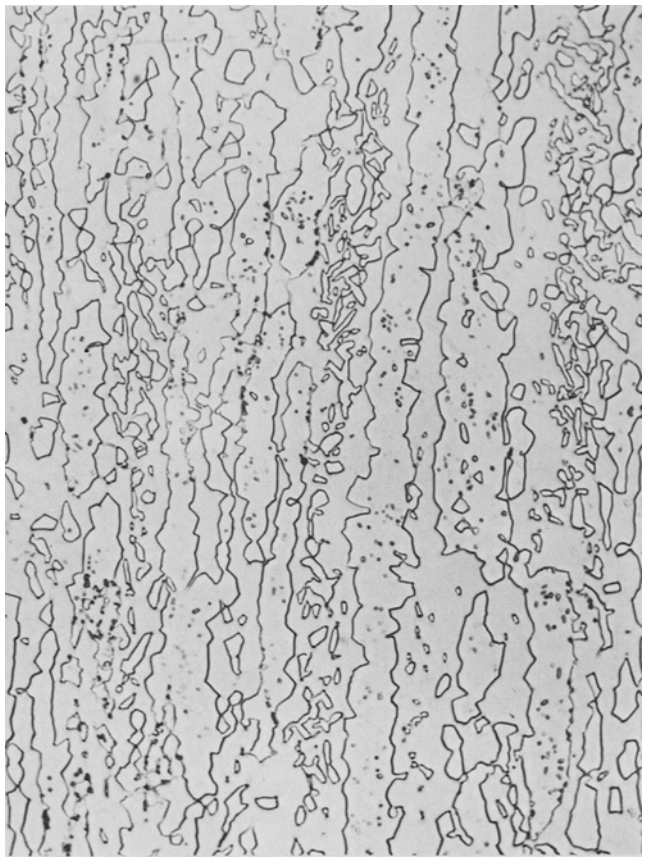

(a)

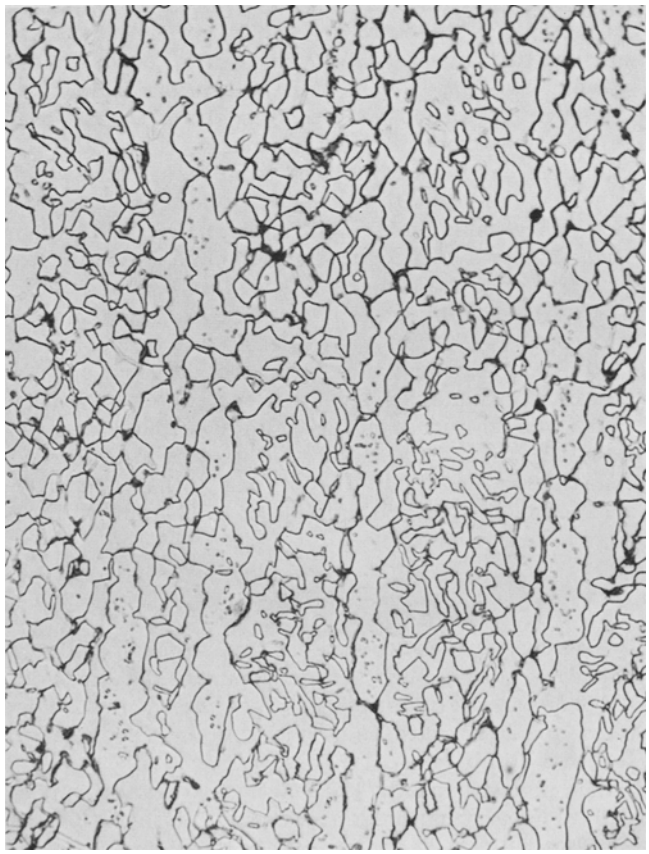

(b)

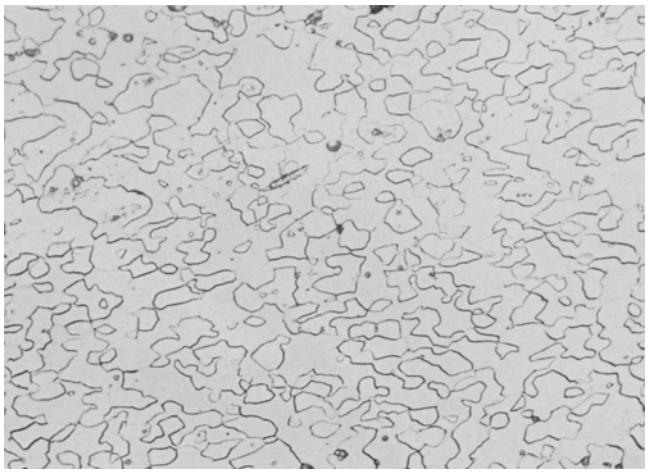

(c)

Fig. 10—Microstructures from a tensile sample of IN-744 deformed at 1700°F having an originally elongated grain structure. (*a*) Grip section, magnification 844 times; (*b*) flange section, magnification 844 times; (*c*) gage section, magnification 634 times. Etched in 10 pct oxalic acid electrolytically.

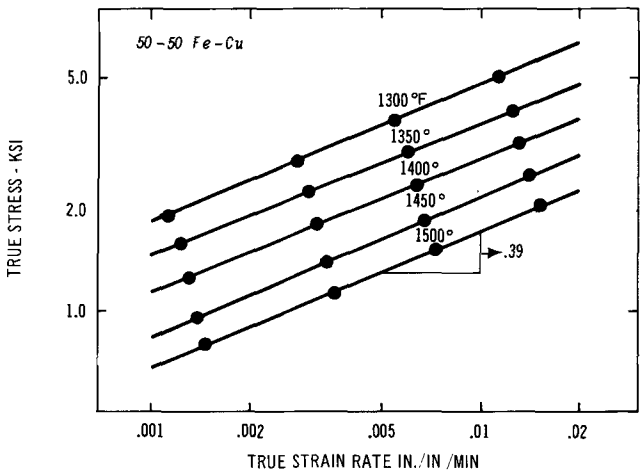

Fig. 11—Stress-strain rate data for an Fe-Cu alloy having an elongated grain structure.

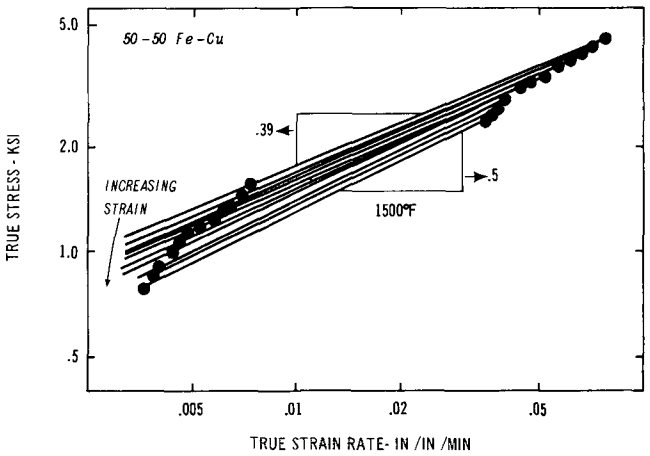

Fig. 12—Change in deformation behavior with increasing strain of a sample of Fe-Cu having an originally elongated grain structure.

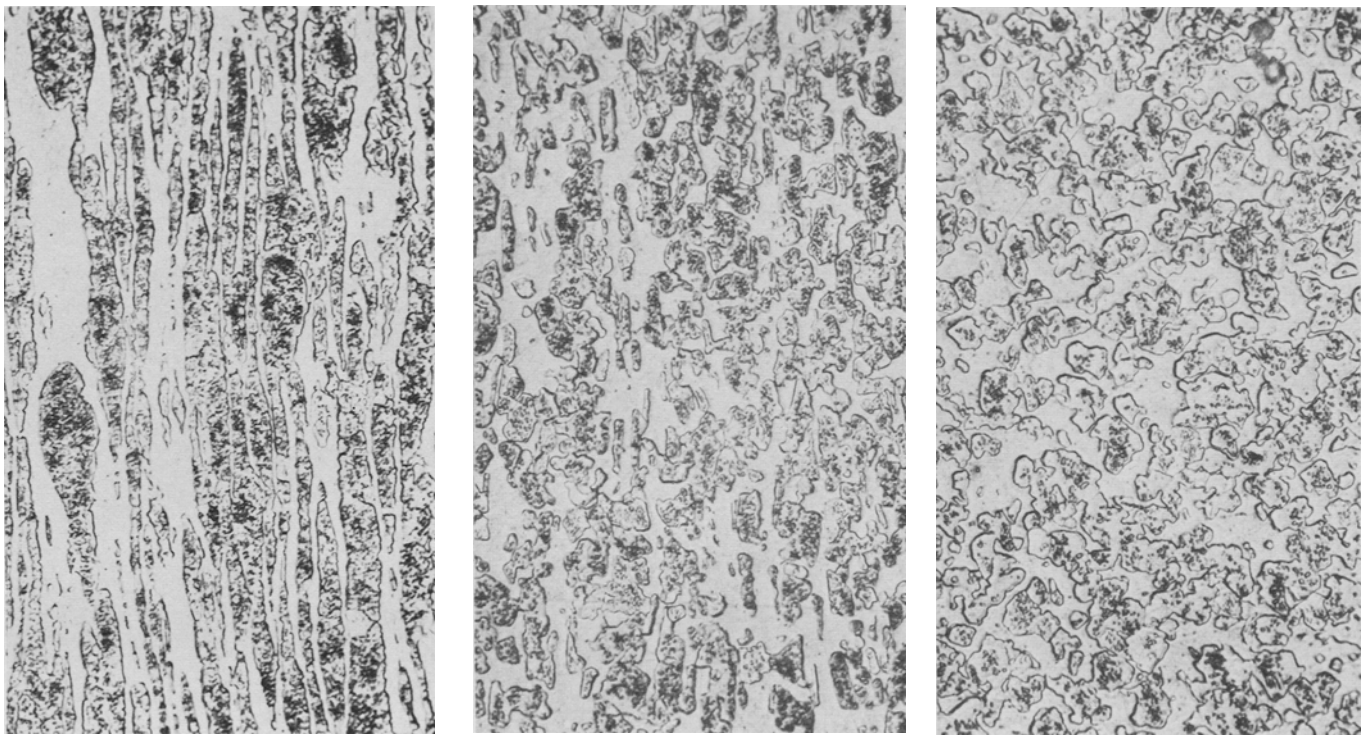

(a) (b) (c)

Fig. 13—Microstructures from a tensile sample of Fe-Cu deformed at 1500° F having an originally elongated grain structure. (*a*) Grip section; (*b*) flange section; (*c*) gage section. Etched in 1 pct nital, magnification 1030 times.

Table III. Predicted and Experimentally Observed Strain Rates for Several Superplastic Alloys

Alloy	T°K	σ, ksi	d, cm X 10^4	b, cm X 10^8	μ, ksi X 10^3	Q, kcal/mole	D, $cm^2/sec.$ X 10^{11}	$\dot{\epsilon}$ - min^{-1} Predicted	$\dot{\epsilon}$ - min^{-1} Observed	Mechanism
Ni-Cr-Fe*	1256	1	2.8	2.5	11.5	60(15)†	3.8	1.2×10^{-2}	1.2×10^{-2}(15)†	*V*
Ni-Cr-Fe	1256	1	4.8	2.5	11.5	61	3.0	3.1×10^{-3}	3.5×10^{-3}	*V*
Ni-Cr-Fe	1033	10	4.8	2.5	11.5	61	0.014	1.7×10^{-3}	1.7×10^{-3}	*V*
Ni-Cr-Fe	1033	10	4.8	2.5	11.5	36	56	1.8×10^{-3}	1.7×10^{-3}	*P*
IN-744	1198	1	3 7	2.5	11.1	60	1.18	2.3×10^{-3}	2.2×10^{-3}	*V*
Sn-Pb	298	1	2.46	3.2	2.5	11(20)	17.8	1.6×10^{-2}	1.38×10^{-2}(2)	*P*
Sn-Bi	298	1	2.3	3.2	2.5	11(20)	17.8	1.9×10^{-2}	3×10^{-3}(6)	*P*
Zn-Al	523	1 42	2.5	2.7	4.9	26	1.4	7.8×10^{-2}	6×10^{-2}(10)	*V*
Zn-Al	523	1.42	2 5	2.7	4.9	23(37)	25	1.39	6×10^{-2}(10)	*V*
Zn-Al	423	1.42	2 5	2.7	4.9	16.5	6	1.9×10^{-3}	6×10^{-4}(10)	
Zn-Al	423	1.42	2.5	2.7	4.9	14.5(10)	66	2×10^{-2}	6×10^{-4}(10)	*P*
Al-Cu	793	1	1 7	2.8	3.7	40(11)	1	5.2×10^{-2}	2.4×10^{-2}(11)	*V*
Ti-Al-V	1223	1	6 6	2.9	6.0	57.5(17)	5.6	8.3×10^{-3}	1.8×10^{-2}(17)	*V*

*Basis for calculation of K_1.

†Parentheses refer to Ref. number.

boundary sliding and dislocation creep may be evaluated. This is done in Table III, starting with data from a Ni-Cr-Fe alloy reported in Ref. 15 and assuming mechanism 4 of Table I. Thus if the grain boundary sliding rate is much greater than the rate of dislocation creep, the locking or friction stress is much less than the applied stress, and the vacancy creep rate is negligible, the deformation behavior should be closely approximated by the equation

$$\dot{\gamma} = \frac{6\pi(1 - \nu)K_1 D_V \sigma^2 b^2}{10 d^2 \mu k T} \qquad [26]$$

Substitution of the quantities shown in Table III leads to a calculated value for K_1 of 0.015 cm. This would suggest, Eq. [4], that at a grain size of 2.8 μ the grain boundary sliding strain rate is over 50 times greater than the dislocation creep rate.

Using this value of K_1, calculations based on either the volume diffusion or pipe diffusion mechanism have been made for various superplastic alloys. The choice of mechanism was based on reported grain size exponents and/or activation energies. With the exception of the Zn-Al system, the predicted and observed strain rates are well within order of magnitude agreement. In the case of Zn-Al, activation energies ranging from 33 to 14 kcal/mole[10,20,22] have been reported in the literature. It can be seen in Table III that activation energies within this range can lead to reasonably accurate predictions. In all cases the room temperature value of the shear modulus of the major component of each

alloy has been employed. Similarly, values of 1.0 and 0.02 cm^2/sec have been used for the preexponential factors for volume and pipe diffusion. More accurate values of any of these factors should lead to no more than an order of magnitude difference in any of the strain rate predictions.

The analysis presented in this paper offers a way of rationalizing a decreasing strain rate exponent with decreasing stress by the inclusion of a locking or friction stress, σ_0. Thus the presence or absence of any apparent low strain-rate exponent domain at low stresses depends on the magnitude of σ_0. It is likely that in any given alloy σ_0 might vary both with grain size and temperature. If σ_0 is very small, there would be a direct transition from the grain boundary sliding-dislocation creep mechanism ($m = 0.5$) to a vacancy creep mechanism ($m = 1$) at low stresses. If σ_0 is an appreciable stress, there would be a two-stage transition of strain-rate exponents from 0.5 to a value which could approach zero and then to 1.0 with decreasing stress.

CONCLUSIONS

1) For various conditions of stress and temperature there are various deformation mechanisms which can be rate-controlling during superplastic deformation.

2) At low stress levels vacancy creep can be both the predominant and rate-controlling process.

3) At intermediate stresses, although grain boundary sliding is the predominant deformation process, its rate and hence the overall deformation rate is controlled by the rate of intragranular dislocation creep.

4) At temperatures between approximately 40 and 65 pct of the melting point dislocation pipe diffusion should be rate-controlling for dislocation creep and consequently grain boundary sliding.

5) At temperatures above about 65 pct of the melting point, volume diffusion should be rate-controlling for both vacancy creep and dislocation creep.

6) The dependence of strain rate on stress and grain size should be different in materials having fine elongated grain structures than in materials having fine equiaxed structures.

7) The present experimental results as well as those for other superplastic alloys are in qualitative and quantitative agreement with the predictions of the analysis presented in this paper.

REFERENCES

1. C. E. Pearson: *J. Inst. Metals,* 1934, vol. 54, p. 111.
2. D. H. Avery and W. A. Backofen: *Trans. ASM,* 1965, vol. 58, p. 551.
3. H. E. Cline and T. H. Alden: *Trans. TMS-AIME,* 1967, vol. 239, p. 710.
4. S. W. Zehr and W. A. Backofen: *Trans. ASM,* 1968, vol. 61, p. 300.
5. T. H. Alden: *Trans. ASM,* 1968, vol. 61, p. 559.
6. T. H. Alden: *Acta Met.,* 1967, vol. 15, p. 469.
7. A. A. Bochvar and Z. A. Sviderskaia: *Izv. Akad. Nauk, SSSR, Otd. Tekh. Nauk,* 1945, vol. 9, p. 821.
8. W. A. Backofen, I. R. Turner, and D. H. Avery: *Trans. ASM,* 1964, vol. 57, p. 980.
9. C. M. Packer and O. D. Sherby: *Trans ASM,* 1967, vol. 60, p. 21.
10. A. Ball and M. Hutchison: *Metal Sci. J.,* 1969, vol. 3, p. 1.
11. D. L. Holt and W. A. Backofen: *Trans. ASM,* 1966, vol. 59, p. 755.
12. D. Lee: *Acta Met.,* 1969, vol. 17, p. 1057.
13. R. C. Gibson, H. W. Hayden, and J. H. Brophy: *Trans. ASM,* 1968, vol 61, p. 85.
14. W. B. Morrison: *Trans. ASM,* 1968, vol. 61, p. 423.
15. H. W. Hayden, R. C. Gibson, H. F. Merrick, and J. H. Brophy *Trans. ASM,* 1967, vol. 60, p. 3.
16. H. W. Hayden and J. H. Brophy: *Trans. ASM,* 1968, vol. 61, p. 542.
17. D. Lee and W. A. Backofen: *Trans. TMS-AIME,* 1967, vol. 239, p. 1034.
18. E. W. Hart: *Acta Met.,* 1967, vol. 15, p. 1545.
19. R. C. Gifkins: *J. Inst. Metals,* 1967, vol. 95, p. 373.
20. T. H. Alden: *J. Aust. Inst. Metals,* 1969, vol. 14, p. 207.
21. T. H. Alden: *Acta Met.,* 1969, vol. 17, p. 1434.
22. P. Chaudhari: *Acta Met.,* 1967, vol. 15, p. 1777.
23. F. R. N. Nabarro: *Proc. Conf. on Strength of Solids,* p. 75, Phys. Soc. of London, Cambridge, 1948.
24. C. Herring: *J. Appl. Phys.,* 1950, vol. 21, p. 437.
25. R. L. Coble: *J. Appl. Phys.,* 1963, vol. 34, p. 1679.
26. I. M. Lifshitz: *Sov. Phys. JETP,* 1963, vol. 17, p. 909.
27. O. D. Sherby and P. M. Burke: *Progr. Mater. Sci.,* 1967, vol. 13, p. 325
28. R. Raj and M. F. Ashby: *Met. Trans.,* 1971, vol. 2, p. 1113.
29. R. N. Stevens *Met. Rev.,* 1966, vol. 11, p. 129.
30. D. McLean and R. C. Gifkins: *J. Inst. Metals,* 1960-61, vol. 89, p. 2.
31. T. S. Kê: *Phys. Rev.,* 1948, vol. 73, p. 267, and *J. Appl Phys.,* 1949, vol. 20, p. 274.
32. J. Friedel: *Dislocations,* Addison Wesley, Cambridge, Mass., 1964.
33. J. Friedel: *Phil. Mag.,* 1955, vol. 46, p. 1169.
34. R. J. Lindinger, R. C. Gibson, and J. H. Brophy: *Trans. ASM,* 1969, vol. 62, p. 230.
35. J. Weertman: *J. Appl. Phys.,* 1955, vol. 26, p. 1213.
36. D. McLean: *Trans. TMS-AIME,* 1968, vol. 242, p. 1193.
37. D. Turnbull and R. E. Hoffman: *Acta Met.,* 1954, vol. 2, p. 419.
38. C. J. Smithells: *Metals Reference Book,* Third Edition, p. 593, Butterworths, Washington, 1962.
39. R. F. Canon and J. P. Stark: *J. Appl. Phys.,* 1969, vol. 40, p. 4366.
40. M. Wuttig and H. K. Birnbaum *Phys. Rev.,* 1966, vol. 147, p. 495.